Sustainability in Environment
ISSN 2470-637X (Print) ISSN 2470-6388 (Online)
Vol. 11, No. 4, 2026
www.scholink.org/ojs/index.php/se

Original Paper

Influence of Ca^{2+} and HCO_3^- and Their Ratios in Water on the Aggregation Behavior of Photosynthetic Bacteria in Karst Regions

Jiaxing Wang[1], Mingliang Wang[1], Jiawang Zhou[1], & Han Wang[1,2*]

[1] College of Eco-Environmental Engineering, Guizhou Minzu University, Guiyang 550025, P.R. China

[2] Guizhou Provincial Engineering Geological Disaster Prevention and Control Engineering Research Center, Guizhou Minzu University, Guiyang 550025, P.R. China

[*] Corresponding Author: Han Wang, E-mail: wanghan1021@gzmu.edu.cn

Guizhou Provincial Basic Research Program (Natural Science) (No. Qiankehe Jichu-ZK [2023] 148)

Received: October 07, 2026 Accepted: November 9, 2026 Online Published: November 24, 2026

doi:10.22158/se.v12n4p170 URL: http://dx.doi.org/10.22158/se.v12n4p170

Abstract

Photosynthetic bacteria (PSB) for organic wastewater treatment represents an innovative approach in anaerobic microbial metabolism and has been applied in aquaculture wastewater. To extend the application scope of this process, the effects of different water bodies must be examined. The water body in karst regions is rich in Ca^{2+}, Mg^{2+}, and HCO_3^-, which may strongly influence the behavior of PSB, particularly their aggregation and extracellular polymeric substances (EPS). The ratios among these ions vary between water bodies. This study investigates the impact of varying ion ratios on the aggregation behavior of PSB, focusing on PSB biomass, EPS, and bacterial micro-morphology. The results demonstrate that different Ca^{2+}/HCO_3^- ratios markedly affect PSB aggregation behavior. The addition of Ca^{2+} and HCO_3^- shortened the lag phase of PSB, and a higher Ca^{2+} proportion (Ca^{2+}/HCO_3^- mass ratio of 4:3) resulted in the strongest aggregation and sedimentation. SEM-EDS analysis revealed Mg- and P-rich crystalline precipitates around the PSB, while Ca was enriched on the bacterial aggregates, suggesting that mineral precipitation and Ca^{2+} bridging jointly facilitated PSB flocculation. The addition of Ca^{2+} and HCO_3^- reduced the protein content of loosely bound EPS (LB-EPS), which may promote bacterial flocculation. Three-dimensional excitation-emission matrix (3D-EEM) fluorescence spectroscopy showed that ion addition increased the proportion of hydrophobic tryptophan-like proteins in LB-EPS, which may further favor PSB flocculation. These findings suggest

that the water in karst regions may be conducive to organic wastewater treatment using PSB, and that the Ca^{2+}/HCO_3^- ratio is a key factor regulating PSB aggregation and solid–liquid separation.

Keywords

Photosynthetic bacteria, Karst region, Aggregation, Ca^{2+}/HCO_3^- ratios, Extracellular polymeric substances

1. Introduction

To achieve carbon neutrality, cost-effective, low-energy, and more environmentally sustainable alternatives for organic wastewater treatment have garnered significant attention [1]. The low-energy advantage of anaerobic treatment of organic wastewater has made it a research hotspot [2,3]. However, traditional anaerobic treatment faces many bottlenecks, such as high land costs, and issues of acid inhibition caused by excessive accumulation of volatile fatty acids, resulting in reduced gas production and lower methane yield [2]. Given the relatively fixed principles of anaerobic biological treatment, coupling processes based on it could be crucial in overcoming these bottlenecks. The coupling with photosynthetic bacteria (PSB) is currently being researched. PSB has already been applied to treat organic wastewater in aquaculture. Since the 1970s, when Masahiro Kobayashi discovered that PSB could treat high-concentration organic wastewater, many scholars have explored using PSB for this purpose [4]. Studies have demonstrated the use of PSB in treating aquaculture wastewater with high organic content [5], brewery wastewater [6], sugar industry wastewater [7], domestic wastewater [8], and livestock wastewater [9]. PSB-based wastewater treatment has numerous advantages over other methods, such as high organic load capacity, small land area requirement, low cost, low energy consumption, non-toxicity, and high pollutant removal efficiency [4]. Using PSB for high-concentration organic wastewater treatment can achieve COD removal rates of 85%–93% and ammonia nitrogen removal rates of 99% [10,11].

However, the influence of regional differences in water chemistry on PSB-based treatment is often overlooked. In karst areas, characterized by groundwater flowing through soluble carbonate and evaporite rocks, high concentrations of Ca^{2+}, Mg^{2+}, and HCO_3^- are present. The karst groundwater mainly contains Ca^{2+} and Mg^{2+}, with Ca^{2+} being the most abundant, and HCO_3^- as the primary anion [12]. The concentration of HCO_3^- is much higher than that of Ca^{2+} and Mg^{2+}. According to Li et al. [13], the average concentrations of Ca^{2+}, Mg^{2+}, and HCO_3^- in the karst groundwater of Guilin, Guangxi, China, during the wet, normal, and dry seasons are 88.24 mg/L, 25.21 mg/L, and 216.57 mg/L, respectively. In the study by Li et al. [14] in the Huanglong Nature Reserve of Sichuan, China, the average concentrations of Ca^{2+}, Mg^{2+}, and HCO_3^- in karst water were 99.73±26.90 mg/L, 8.54±2.21 mg/L, and 308.88±87.72 mg/L, respectively. Wang et al. [12] reported average concentrations of Ca^{2+}, Mg^{2+}, and HCO_3^- of 66.7 mg/L, 33.4 mg/L, and 313 mg/L, respectively. Because HCO_3^- governs the inorganic carbon balance and pH of the water, and the CO_3^{2-} derived from HCO_3^- can precipitate with Ca^{2+} under non-acidic conditions, the dosing of PSB may interact strongly with these ions. Moreover,

PSB secrete abundant extracellular polymeric substances (EPS), which can bind divalent cations and thereby affect cell aggregation. Few studies have investigated the effects of these ions on the treatment of organic wastewater using PSB.

The study aims to culture *Rhodopseudomonas palustris* in simulated karst water and investigate the effects of varying Ca^{2+} and HCO_3^- ratios on the growth and aggregation of the bacteria. A UV-visible spectrophotometer (UV) was used to measure the daily growth of photosynthetic bacteria in the culture bottles. After extracting loosely bound extracellular polymeric substances (LB-EPS), a microplate reader was utilized to determine the LB-EPS protein concentration under different media and inoculation amounts. Scanning electron microscopy (SEM) and energy dispersive spectroscopy (EDS) were employed to analyze the morphology and elemental composition of the precipitates formed in the *Rhodopseudomonas palustris* cultures, and three-dimensional excitation-emission matrix (3D-EEM) fluorescence spectroscopy was used to characterize the LB-EPS components.

2. Materials and Methods

2.1 Photosynthetic Bacteria

A high-speed benchtop centrifuge (GT10-1, Beili, Beijing, China) was used to centrifuge the *Rhodopseudomonas palustris* bacterial suspension at 5000 rpm for 10 minutes. The supernatant was aspirated, and the bacterial pellet was washed with phosphate-buffered saline (PBS, pH 7.0). The sample was centrifuged again for 10 minutes (the washing was repeated two to three times), and the resulting bacterial pellet was collected and stored for future use in culturing experiments. Before inoculation, the pellet was resuspended and the OD_{660} of the suspension was adjusted to 0.6.

2.2 Photosynthetic Bacteria Medium

Calcium ions (Ca^{2+}) and bicarbonate ions (HCO_3^-) were added to a standard culture medium to simulate karst region groundwater, creating several media with different Ca^{2+} to HCO_3^- ratios. The composition of the standard culture medium includes 2.5 g of sodium acetate (CH_3COONa), 0.2 g of magnesium sulfate heptahydrate ($MgSO_4 \cdot 7H_2O$), 2.0 g of yeast extract, 1.0 g of ammonium chloride (NH_4Cl), 0.5 g of potassium dihydrogen phosphate (KH_2PO_4), and 1000 mL of sterile water.

To this base medium, different proportions of calcium chloride ($CaCl_2$) and potassium bicarbonate ($KHCO_3$) were added. One set of media contained 0.22 g of $CaCl_2$ and 0.2 g of $KHCO_3$, resulting in a Ca^{2+} concentration of 80 mg/L and an HCO_3^- concentration of 120 mg/L, with a Ca^{2+} to HCO_3^- ratio of 2:3 (mass concentration ratio). Another set contained 0.44 g of $CaCl_2$ and 0.2 g of $KHCO_3$, resulting in a Ca^{2+} concentration of 160 mg/L and an HCO_3^- concentration of 120 mg/L, with a Ca^{2+} to HCO_3^- ratio of 4:3. The compositions of the three media are listed in Table 1.

Table 1. Composition of the Photosynthetic Bacteria Culture Media (Ca^{2+}/HCO_3^- ratios are mass concentration ratios)

Component	No added Ca^{2+} and HCO_3^-	Ca^{2+}/HCO_3^- = 2:3	Ca^{2+}/HCO_3^- = 4:3
CH_3COONa	2.5 g	2.5 g	2.5 g
$MgSO_4 \cdot 7H_2O$	0.2 g	0.2 g	0.2 g
Yeast extract	2.0 g	2.0 g	2.0 g
NH_4Cl	1.0 g	1.0 g	1.0 g
KH_2PO_4	0.5 g	0.5 g	0.5 g
Sterile water	1000 mL	1000 mL	1000 mL
$CaCl_2$	–	0.22 g	0.44 g
$KHCO_3$	–	0.2 g	0.2 g

–, not added.

After preparation, the media were sterilized at 121 °C for 20 minutes. To prevent precipitation during sterilization, a $CaCl_2$ stock solution sterilized by filtration through a 0.22 μm membrane was added in a clean bench after the media had cooled.

2.3 Cultivation Expansion of Photosynthetic Bacteria

The bacterial suspension (OD_{660} = 0.6) and pre-prepared photosynthetic bacterial culture medium were added to transparent, sealed cell culture bottles (NEST, Wuxi, China). Each medium was inoculated at 15% and 20%, giving six treatments: A and B (no added Ca^{2+} and HCO_3^-), C and D (Ca^{2+}/HCO_3^- = 2:3), and E and F (Ca^{2+}/HCO_3^- = 4:3), with A, C and E inoculated at 15% and B, D and F at 20%.

A full-spectrum Ra98 low-voltage LED light strip (24 V DC, 24 W) was installed above the water bath shaker to ensure even illumination throughout the shaker. The cell culture bottles were placed in the water bath shaker, set to a temperature of 30 °C and a shaking speed of 80 rpm. The LED light strip provided an intensity of 5000 lux at the liquid surface of the water bath.

Samples were taken from each cell culture bottle every 24 hours. The absorbance at 660 nm was measured using a UV-Vis spectrophotometer (TU-1950, Persee, Beijing, China) [15]. Additionally, 0.7 mL of the bacterial culture was extracted from the medium and stored at 4 °C.

2.4 Microscopic Characterization of Photosynthetic Bacterial Aggregation Behavior Using Scanning Electron Microscope (SEM) and Energy Dispersive Spectrometer (EDS)

To observe the distribution and morphological characteristics of adsorbates around the bacterial strains, SEM (Sigma 300, Zeiss, Oberkochen, Germany) and EDS (XFlash 6-30, Bruker, Berlin, Germany) were utilized. Precipitates from the bottoms of various culture media were collected and vacuum-dried before being sputter-coated with gold.

The SEM was employed to observe photosynthetic bacteria's distribution and morphological features

and surrounding adsorbates in the samples. Specific areas of interest were delineated for EDS analysis, which provided data on the compositional elements of the adsorbates. This combined analysis yielded information on the morphological characteristics of the adsorbates in the bacterial culture, the distribution of photosynthetic bacteria and adsorbates, and the elemental composition of the adsorbates.

2.5 Extraction and Determination of LB-EPS

The extraction method of LB-EPS was conducted as per previous studies [16]. The bacterial cells collected each day were pelleted by centrifugation and resuspended in 7 mL of 0.9% NaCl solution. Subsequently, ultrasonic oscillation using an ultrasonic homogenizer (JY92-IIN, Scientz, Ningbo, China) at 20 kHz was applied for 2 minutes, followed by horizontal shaking at 150 rpm for 10 minutes and another 2 minutes of ultrasonic oscillation. The photosynthetic bacteria and the supernatant were separated using the high-speed benchtop centrifuge described in Section 2.1 at 5000 × *g* for 15 minutes. The supernatant was then extracted using a syringe, passed through a 0.22 μm membrane filter, and regarded as LB-EPS.

The protein concentration in the LB-EPS extract was determined using a multi-mode microplate reader (Synergy H1, BioTek, Winooski, VT, USA). Under alkaline conditions, proteins in the sample reduced Cu^{2+} to Cu^{+}, which formed a purple-blue complex with the BCA reagent (BCA Protein Assay Kit, PC0020, Solarbio, Beijing, China). The absorbance at 562 nm was measured [17], and the protein concentration of the sample was calculated using a standard curve [18].

2.6 Integration of 3D-EEM and FRI for Fluorescence Spectroscopy

EEM spectra are collections of emission spectra over a range of excitation wavelengths, which can identify fluorescent compounds in complex mixtures [19].

EEM spectra were recorded with a fluorescence spectrophotometer (RF-6000, Shimadzu, Kyoto, Japan) operated with LabSolutions RF software (version 1.17). In this study, excitation wavelengths were varied from 200 nm to 450 nm in 5 nm increments, and emission wavelengths ranged from 250 nm to 600 nm in 1 nm increments. The scanning speed was set at 6000 nm/min, the excitation and emission slit widths were both 5 nm, and the sensitivity was set to low, with distilled water as the blank sample for spectral recording, and all measurements were performed at a constant temperature of 25 °C.

The X-axis represents excitation wavelengths from 200 nm to 450 nm, and the Y-axis represents 250 nm to 600 nm emission wavelengths. Origin software (OriginLab, Northampton, MA, USA) was used to process the EEM data. The EEM data were exported in CSV format, the fluorescence volume of each region was obtained by double integration over the excitation and emission wavelengths, missing values caused by the detection range of the instrument were filled by interpolation, and the fluorescence volume of each region was normalized to the total fluorescence volume.

Different organic compounds have distinct excitation and emission wavelengths. According to studies [20,21], EEM data were divided into five characteristic regions and a remaining area (Region VI) (Table 2).

Table 2. Excitation/Emission (Ex/Em) Wavelength Ranges of the Fluorescence Regions Used in FRI Analysis [20,21]

Region	Fluorescent substance	Ex/Em (nm)
Region I	Tyrosine-like proteins	200–250/280–330
Region II	Tryptophan-like proteins	200–250/330–380
Region III	Fulvic acid-like substances	200–250/380–550
Region IV	Soluble microbial by-product-like substances	250–280/280–380
Region V	Humic acid-like substances	250–400/380–550
Region VI	Remaining area not assigned to Regions I–V	Other Ex/Em

The fluorescence intensities at various excitation-emission wavelengths were normalized to the relative area, expressed as (1) individual region values, (2) overall region values, and (3) fluorescence response percentages. I($\lambda_{ex}\lambda_{em}$) represents the fluorescence intensity at various excitation-emission wavelengths, where $\Delta\lambda_{ex}$ denotes the excitation wavelength increment of 5 nm, and $\Delta\lambda_{em}$ signifies the emission wavelength increment of 1 nm. MF_i stands for the multiplication factor for each region, specifically the derivative of fractional projection of excitation-emission areas [22,23].

$$\phi_{\text{in}} = MF_{\text{i}}\phi_{\text{i}} = MF_{\text{i}} \sum_{ex} \sum_{em} I(\lambda_{ex}\lambda_{em})\Delta\lambda_{ex}\Delta\lambda_{em} \tag{1}$$

$$\phi_{\text{Tn}} = \sum \phi_{\text{in}} \tag{2}$$

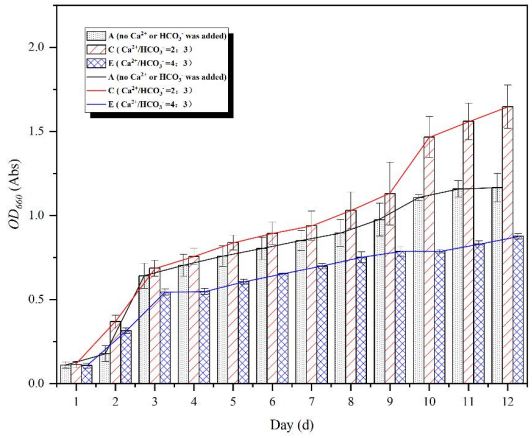
$$P_{i,n} = \phi_{in} / \phi_{Tn} \times 100\% \tag{3}$$

2.7 Data Analysis

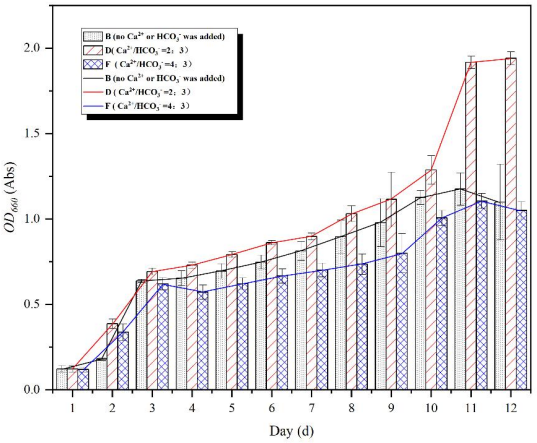
All cultivation experiments were performed in triplicate, and the growth data are presented as mean ± standard deviation (n = 3).

3. Results

3.1 Growth of Photosynthetic Bacteria



(a) The inoculation amount of photosynthetic bacteria in the culture medium is 15%.

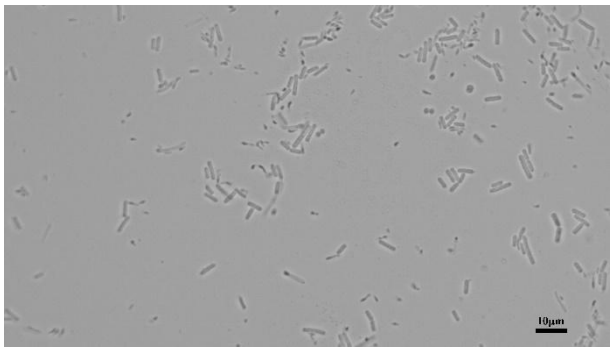


(b) The inoculation amount of photosynthetic bacteria in the culture medium is 20%.

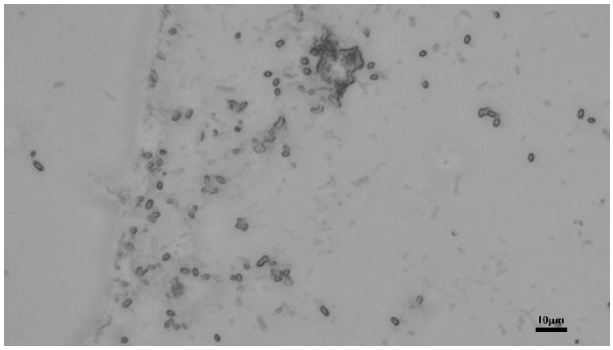
Figure 1. Growth (OD_{660}) of photosynthetic bacteria with inoculation amounts of 15% (a) and 20% (b): without the addition of Ca^{2+} and HCO_3^- (A, B); with the addition of Ca^{2+} and HCO_3^- in a ratio of 2:3 (C, D); and with the addition of Ca^{2+} and HCO_3^- in a ratio of 4:3 (E, F). Error bars represent standard deviations (n = 3).

The growth of photosynthetic bacteria in the six treatments over 12 days is shown in Figure 1. From the bar-line chart, it can be observed that for *Rhodopseudomonas palustris*, the growth is better at an inoculation level of 20% compared to 15%. Regarding the types of culture media, the medium supplemented with Ca^{2+} and HCO_3^- reaches the logarithmic phase more quickly, particularly the medium with a Ca^{2+}/HCO_3^- ratio of 2:3. Furthermore, it maintains a higher growth rate even after growth rates in other types of media gradually decline. Overall, the medium with a Ca^{2+}/HCO_3^- ratio of 2:3 showed the highest OD_{660}, followed by the medium without additional ions and the medium with a ratio of 4:3. Figure 1 also shows that groups A and B (culture media without the addition of Ca^{2+} and HCO_3^-) enter the exponential growth phase later than groups C and D (with Ca^{2+}/HCO_3^- = 2:3) and groups E and F (with Ca^{2+}/HCO_3^- = 4:3). It should be noted that the lower OD_{660} values of groups E

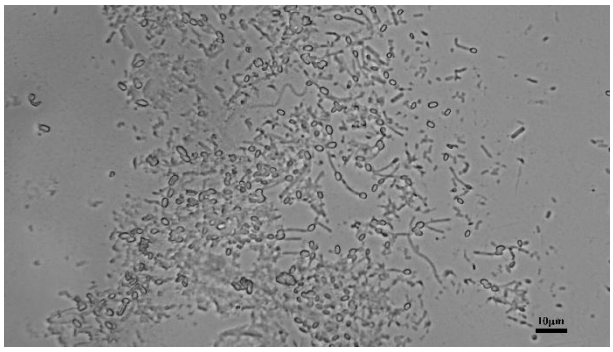
and F partly reflect the strong aggregation and settling of cells in the 4:3 media (Section 3.2), which causes turbidity-based measurements to underestimate the biomass; therefore, OD_{660} alone cannot be used to compare the biomass of the 4:3 groups with that of the other groups.



(a) Without the addition of Ca^{2+} and HCO_3^-



(b) Ca^{2+}/HCO_3^- = 2:3



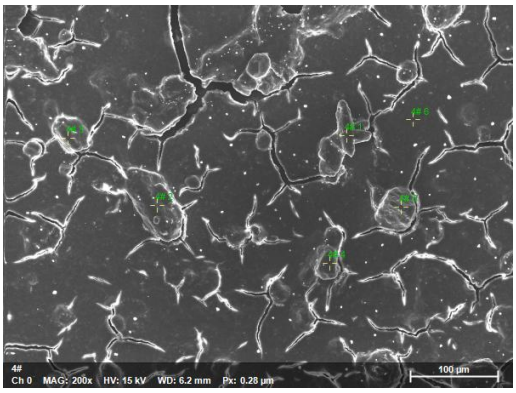
(c) Ca^{2+}/HCO_3^- = 4:3

Figure 2. Photosynthetic bacteria in the culture medium observed under an optical microscope with a 100× oil-immersion objective: (a) culture medium without the addition of Ca^{2+} and HCO_3^-; (b) culture medium with Ca^{2+}/HCO_3^- = 2:3; (c) culture medium with Ca^{2+}/HCO_3^- = 4:3. Scale bar = 10 μm

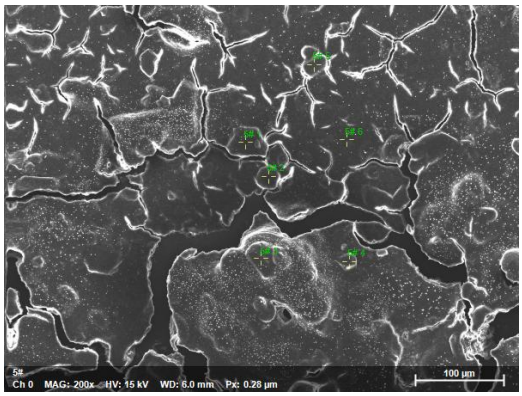
During the cultivation of photosynthetic bacteria, if cell culture bottles are left standing for some time, a reddish precipitate can be observed at the bottom of bottles supplemented with Ca^{2+} and HCO_3^-, as

shown in Figure 2. In contrast, no reddish precipitate forms in the medium without additional ions. A micropipette was used to extract some of the bottom precipitates, and bacterial colonies were examined under an optical microscope (UB203i-NZ, UOP, Chongqing, China) with a 40× objective. The microscope was then adjusted to use an oil immersion lens with a drop of cedar oil in the sample area to observe bacterial colonies with a 100× objective. Figure 2(b) and 2(c) show large crystal-like bright spots around bacterial cells in the medium supplemented with Ca^{2+} and HCO_3^-. Some bright spots completely cover bacterial cells, while others are adsorbed around bacterial cells. Moreover, the medium with a Ca^{2+}/HCO_3^- ratio of 4:3 shows more bacterial cells and bright spots compared to the medium with a Ca^{2+}/HCO_3^- ratio of 2:3, indicating stronger cell–crystal aggregation. As shown in Figure 2(a), no bright spots appear in the medium without additional ions, and only bacterial cells are observed.

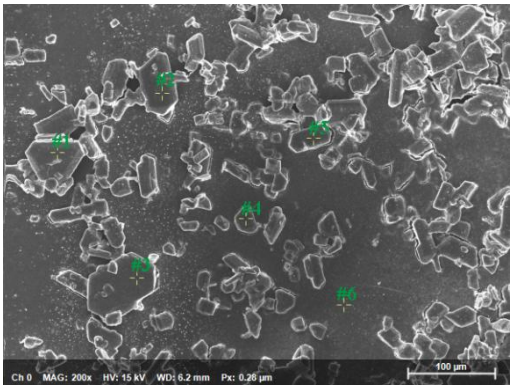
3.2 SEM-EDS Characterization of the Precipitates



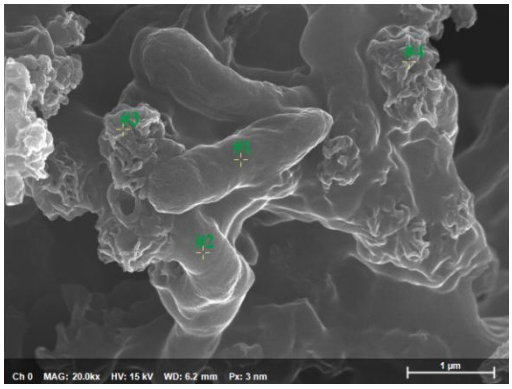
(a) Ca^{2+}/HCO_3^- = 2:3



(b) Ca^{2+}/HCO_3^- = 4:3



(c) Ca^{2+}/HCO_3^- = 4:3, EDS points on crystals (200×)



(d) Ca^{2+}/HCO_3^- = 4:3, EDS points on bacterial clusters (20.0 k×)

Figure 3. SEM images of the precipitates formed with the addition of Ca^{2+} and HCO_3^- in a ratio of 2:3 (a); addition of Ca^{2+} and HCO_3^- in a ratio of 4:3 (b); EDS analysis points on the crystals (c, 200×) and on the bacterial clusters (d, 20.0 k×) in the 4:3 medium, numbered as in Table 3. The pale yellow cross marks the sampling points where the bacteria flocculated and combined with the crystals

The crystal-containing precipitate at the bottom of the media supplemented with Ca^{2+} and HCO_3^- was analyzed using a Scanning Electron Microscope (SEM) and Energy Dispersive Spectrometer (EDS). The SEM images revealed the crystals' distribution and morphological characteristics around the photosynthetic bacteria. As shown in Figure 3(a) (Ca^{2+}/HCO_3^- = 2:3), numerous geometric crystals were formed, with some overlapping crystals and others adsorbed around the bacteria.

EDS point analysis was performed on the crystals selected in the SEM images. When the EDS point scan was focused on the crystals, high contents of C, O, and P and smaller amounts of Ca and Mg were observed. Because C and O also originate from the bacterial cells and organic matter in the medium, whereas P was abundant at the crystal points (the medium contained KH_2PO_4), the crystals are most likely Ca- and Mg-bearing phosphate precipitates, possibly mixed with $CaCO_3$ and $MgCO_3$.

For the 4:3 medium (Figure 3(b)–(d)), EDS point scans were also performed on the crystals and bacterial clusters. As shown in Table 3a, the crystals contained high contents of C, O, and P and a smaller amount of Mg. No Ca was detected at the crystal points (Figure 3(c); Table 3a), whereas Ca (13.33–19.49 wt%) was detected at the bacterial cluster points analyzed at 20.0 k× (Figure 3(d); Table 3b). This suggests that the crystals in this medium were mainly Mg-bearing phosphates, whereas Ca was mainly associated with the bacterial aggregates, where it may bridge EPS and promote flocculation.

Table 3. Normalized Mass Percentages (wt%) of Elements at the EDS Points of the Precipitate Formed in the Medium with Ca^{2+}/HCO_3^- = 4:3: (a) crystal points (200×); (b) bacterial cluster points (20.0 k×)

Point	C	O	Na	Mg	Si	P	Cl	K	Ca
(a) Crystal points (200×)									
#1	43.60	21.67	n.d.	10.42	n.d.	22.57	1.73	n.d.	n.d.
#2	47.60	18.52	1.40	9.05	n.d.	20.49	2.95	n.d.	n.d.
#3	50.41	18.13	1.15	8.71	n.d.	19.99	1.62	n.d.	n.d.
#4	29.10	34.46	2.39	12.48	n.d.	19.89	1.01	n.d.	n.d.
#5	31.59	30.75	2.29	12.35	n.d.	21.74	1.27	n.d.	n.d.
#6	43.61	43.72	12.66	n.d.	n.d.	n.d.	n.d.	n.d.	n.d.
Mean	40.99	27.88	3.98	10.60	–	20.94	1.72	–	–
SD	8.67	10.24	4.89	1.78	–	1.17	0.75	–	–
SE	3.54	4.18	1.99	0.73	–	0.48	0.30	–	–
(b) Bacterial cluster points (20.0 k×)									
#1	26.12	41.29	3.14	1.44	n.d.	11.33	1.09	0.75	14.83
#2	38.29	35.91	1.81	0.86	n.d.	8.09	1.11	0.60	13.33
#3	25.75	38.46	2.19	1.35	n.d.	10.85	1.02	0.90	19.49
#4	27.24	39.45	2.71	1.24	0.65	12.31	0.90	n.d.	15.49
Mean	29.35	38.78	2.46	1.22	0.65	10.65	1.03	0.75	15.79
SD	5.99	2.24	0.58	0.25	0.00	1.81	0.10	0.15	2.63
SE	3.00	1.12	0.29	0.13	0.00	0.90	0.05	0.07	1.31

Point numbers correspond to those in Figure 3(c) and 3(d). Mean, SD and SE were calculated by the EDS software; elements not detected at any point were not averaged. n.d., not detected; SD, standard deviation; SE, standard error of the mean; –, not calculated.

When the ratio of Ca^{2+}/HCO_3^- was 4:3, the crystals and many bacterial clusters might have adsorbed too densely, resulting in an uneven distribution of photosynthetic bacteria in the solution. Consequently, the photosynthetic bacteria in the liquid sample in the cuvette were also unevenly distributed, leading to low daily absorbance measurements.

Combined with the optical microscope images (Figure 2), the settled precipitate in the 4:3 medium, where Mg-bearing phases dominated, contained more bacterial aggregates than that in the 2:3 medium, where both Ca- and Mg-bearing precipitates formed. Thus, when adding Ca^{2+} and HCO_3^-, controlling their ratio to 4:3 resulted in better precipitation and flocculation than a 2:3 ratio.

3.3 LB-EPS Protein Content

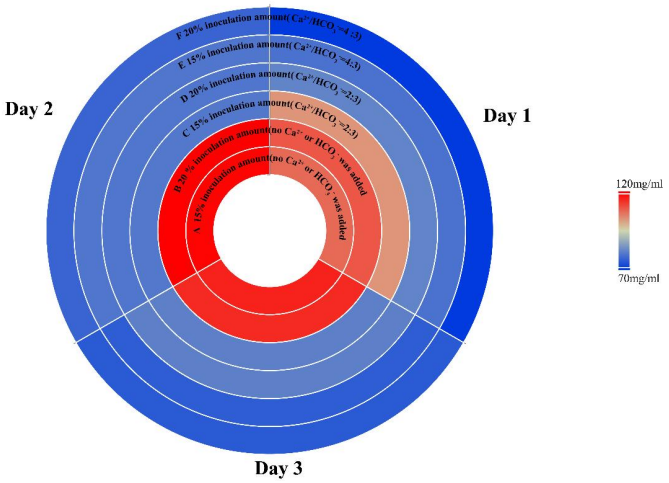
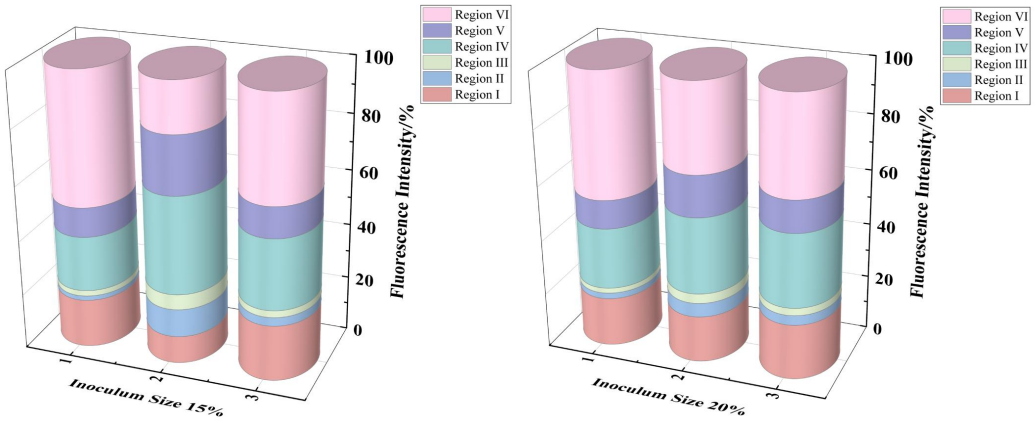


Figure 4. Protein concentration of LB-EPS from photosynthetic bacteria during the exponential growth phase. A and B are media without added Ca^{2+} and HCO_3^-; C and D are media with a Ca^{2+} to HCO_3^- ratio of 2:3; E and F are media with a Ca^{2+} to HCO_3^- ratio of 4:3

The protein concentrations of LB-EPS are shown in Figure 4. It can be observed that during the exponential growth phase, the protein concentrations of media groups A and B, which did not have extra ions added, were higher over three days than those of media groups C, D, E, and F, which had Ca^{2+} and HCO_3^- added. Higher LB-EPS content is generally associated with poorer flocculation. Studies have shown that excessive LB-EPS alters the surface charge and hydrophobicity of cells, which affects zeta potential and results in poor flocculation performance [24]. Other studies indicate that increased EPS concentration increases surface negative charge, leading to poor self-flocculation ability [25].

Together with the optical microscope observations (Figure 2), these results indicate that adding Ca^{2+} and HCO_3^- reduces the LB-EPS protein content of photosynthetic bacteria, which favors bacterial flocculation.

3.4 Fluorescence Regional Integration (FRI) on the Three-dimensional Excitation Emission Matrix (EEM)



(a) Inoculation amount of 15% (b) Inoculation amount of 20%

Figure 5. The fluorescence response in each region of LB-EPS: (a) inoculation amount of 15%; (b) inoculation amount of 20%. Bars 1–3 represent the media without added Ca^{2+} and HCO_3^-, with Ca^{2+}/HCO_3^- = 2:3 and with Ca^{2+}/HCO_3^- = 4:3, respectively

After performing Fluorescence Regional Integration (FRI) on the three-dimensional excitation-emission matrix (EEM) fluorescence data, the percentages of the total for each region—tyrosine protein-like, tryptophan protein-like, soluble microbial by-product-like, humic-like, and fulvic-like substances—were obtained. The fluorescence responses of the LB-EPS components collected during the exponential growth phase are shown in Figure 5. Region I represents tyrosine-like proteins, Region II tryptophan-like proteins, Region III fulvic acid-like substances, Region IV soluble microbial by-products, Region V humic acid-like substances, and Region VI is the remaining area not assigned to Regions I–V [20]. Because Region VI covers the remaining area of the EEM, the total fluorescence volume corresponds to the whole spectrum, and the percentage of Region II ($P_{i,n}$) therefore depends only on the Region II boundaries (Table 2).

As shown in Figure 5(a), with an inoculation amount of 15%, the tryptophan $P_{i,n}$ in LB-EPS of the medium without extra ions added was 3.18%, while it was 5.12% in the medium with a Ca^{2+}/HCO_3^- ratio of 2:3, and 3.55% in the medium with a Ca^{2+}/HCO_3^- ratio of 4:3. As shown in Figure 5(b), with an inoculation amount of 20%, the tryptophan $P_{i,n}$ in LB-EPS of the medium without extra ions added was 1.66%, while it was 10.17% in the medium with a Ca^{2+}/HCO_3^- ratio of 2:3, and 3.14% in the medium with a Ca^{2+}/HCO_3^- ratio of 4:3.

At different inoculation amounts of photosynthetic bacteria, the tryptophan percentage in the medium with extra ions added is higher than that in the medium without extra ions. Studies have indicated that the proportion of EPS components may have a greater impact on microbial flocculation [26]. Tryptophan is one of the most hydrophobic amino acids, and tryptophan-like proteins can promote cell aggregation through hydrophobic interaction and bridging. Chai et al. [27] found that low levels of tryptophan can worsen particle aggregation, while high levels of tryptophan-induced hydrophobic

attraction play a significant role in particle aggregation. Therefore, the increased proportion of tryptophan-like proteins in LB-EPS after ion addition may contribute to PSB flocculation, together with the mineral precipitates described in Section 3.2.

4. Discussion

Ca^{2+} and HCO_3^- affected both the growth and the flocculation of PSB, and the flocculation response depended strongly on the ion ratio. At the concentrations tested, the addition of Ca^{2+} and HCO_3^- shortened the lag phase, and the medium with a Ca^{2+}/HCO_3^- ratio of 2:3 showed the highest OD_{660}. In contrast, a higher Ca^{2+} proportion (4:3) produced the strongest aggregation and sedimentation; because the dense aggregates lowered the measured OD_{660}, the effect of this ratio on biomass could not be determined from turbidity alone. Flocculation may be due to the formation of Ca- and Mg-bearing (mainly phosphate) precipitates that help bacterial precipitation. Previous studies have shown that the binding between EPS and divalent cations (such as Ca^{2+} and Mg^{2+}) is one of the main intermolecular interactions maintaining the structure of microbial aggregates [28]. It is also possible that high concentrations of Ca^{2+} and Mg^{2+} bridge with EPS, promoting cell flocculation [29,30]. In this study, Ca was not detected in the crystals but accounted for 15.79 wt% on average at the bacterial cluster points (Table 3), suggesting that Ca^{2+} acted mainly by bridging negatively charged groups of EPS on the cell surface, thereby neutralizing surface charge and reducing electrostatic repulsion between cells. Together with the hydrophobic interaction of tryptophan-like proteins (Section 3.4) and the mineral precipitates, these results suggest that PSB flocculation in karst water results from the combined effects of ion bridging, hydrophobic interaction and precipitation, and that the dominant mechanism may shift with the Ca^{2+}/HCO_3^- ratio: at 2:3, the proportion of tryptophan-like proteins was the highest, whereas at 4:3, Ca^{2+} bridging and mineral precipitation appear to dominate. Therefore, regulating the Ca^{2+}/HCO_3^- ratio to enhance the flocculation of photosynthetic bacteria in karst water to treat high concentrations of organic matter is a new research direction. This study also provides new perspectives and data support for optimizing bacterial growth environments and treating high concentrations of organic matter in karst water.

In lakes, the relationship between photosynthetic bacteria and lake depth follows two patterns. The first is that bacterial numbers gradually increase with depth and peak near the bottom. The second is that photosynthetic bacteria primarily grow in a limited, narrow layer between the oxic and anoxic zones [31]. It can therefore be speculated that, in karst water with high concentrations of Ca^{2+} and HCO_3^-, photosynthetic bacteria may flocculate more readily, settling to the bottom or between the oxic and anoxic zones, which may enhance their degradation of pollutants there. This may aid in the removal of bottom sediment pollutants in shallow lakes. Conversely, when PSB are applied to purify surface water, strong flocculation at high Ca^{2+}/HCO_3^- ratios may cause the cells to settle out of the illuminated surface layer and reduce their efficiency; in such cases, immobilization carriers or periodic mixing may be required to keep the cells in suspension.

The findings of this study have potential practical implications for organic wastewater treatment in karst areas. In these regions, the naturally high concentrations of Ca^{2+} and HCO_3^- may give photosynthetic bacteria an inherent advantage in treating high concentrations of organic wastewater. By adjusting the ratio of Ca^{2+} and HCO_3^-, the flocculation of photosynthetic bacteria can be promoted, which may simplify biomass separation and reduce treatment costs and energy consumption, enhancing the economic and environmental benefits of wastewater treatment. This approach has potential for practical applications, especially in treating industrial and domestic wastewater.

Despite these findings, some limitations remain. First, the experimental conditions were strictly controlled in the laboratory, while real-world application environments may be more complex, requiring further validation of these results' universality. Second, the research focused only on the growth and flocculation effects of specific types of photosynthetic bacteria; future studies could expand to other bacterial species to verify their performance under similar conditions. Third, the mineral phases of the precipitates were inferred from EDS point analysis only and should be confirmed by X-ray diffraction (XRD) or Fourier transform infrared spectroscopy (FTIR). Fourth, the Ca^{2+}/HCO_3^- mass ratios tested (2:3 and 4:3) are higher than those of the natural karst waters cited above (approximately 0.2–0.4 [12–14]), so the effects at lower ratios remain to be verified. Fifth, growth was evaluated only by OD_{660}, which is affected by cell aggregation; biomass indicators such as dry cell weight or total cellular protein should be measured in future work. Additionally, future research should explore applying these optimized conditions on a larger scale, including experimental studies in actual wastewater treatment, to ensure feasibility and effectiveness.

5. Conclusion

In cultivating photosynthetic bacteria in a simulated karst water environment, it was found that the addition of Ca^{2+} and HCO_3^- shortened the lag phase of photosynthetic bacteria, and that a higher Ca^{2+} proportion (Ca^{2+}/HCO_3^- mass ratio of 4:3) resulted in the strongest flocculation and sedimentation. First, through optical microscopy and then through scanning electron microscopy-energy dispersive X-ray spectroscopy (SEM-EDS) analysis, crystal structures were identified around photosynthetic bacteria at high concentrations of Ca^{2+} and HCO_3^-, which were mainly Mg- and P-rich (phosphate) precipitates, while Ca was enriched on the bacterial aggregates; mineral precipitation and Ca^{2+} bridging may jointly aid bacterial flocculation and sedimentation. After extracting the loosely bound extracellular polymeric substances (LB-EPS) from the photosynthetic bacteria, a microplate reader was used to quantitatively analyze the protein content. The results showed that adding Ca^{2+} and HCO_3^- reduced the protein content of LB-EPS, which may promote bacterial flocculation. Additionally, three-dimensional excitation-emission matrix (3D-EEM) fluorescence spectroscopy was used to perform fluorescence region integration (FRI) on the LB-EPS, which showed that ion addition increased the proportion of hydrophobic tryptophan-like proteins that may contribute to the flocculation of photosynthetic bacteria. Therefore, the Ca^{2+}/HCO_3^- ratio is a key factor controlling the flocculation of photosynthetic bacteria

and should be considered when applying PSB in karst regions.

6. Implication

This study revealed through systematic experiments the marked effects of different concentrations and combinations of Ca^{2+} and HCO_3^- on photosynthetic bacteria's growth and flocculation efficiency. The addition of Ca^{2+} and HCO_3^- shortened the lag phase of photosynthetic bacteria, and a Ca^{2+}/HCO_3^- ratio of 4:3 favored their flocculation. The study results indicate that optimizing the ratio of Ca^{2+} and HCO_3^- can promote the flocculation of photosynthetic bacteria, providing a basis for developing an economical and environmentally friendly method for organic wastewater treatment in karst regions. Compared to traditional wastewater treatment methods, this biological treatment technology may offer advantages such as low energy consumption and low secondary pollution, making use of the unique aquatic chemistry conditions in karst regions and contributing to sustainable wastewater treatment. Future research should further optimize culture medium compositions and explore more types of photosynthetic bacteria and their performance under different environmental conditions.

Furthermore, it is recommended that the results of this study be validated on a larger scale and under different environmental conditions, especially in practical wastewater treatment applications, to promote the widespread application of this method in practice. Through continuous research and optimization, photosynthetic bacteria are expected to play a greater role in wastewater treatment, promoting its development and innovation. Ammonia nitrogen concentrations are high in organic, high-concentration aquaculture wastewater [32]. The next step could build upon this study to investigate whether magnesium phosphate crystals can precipitate with ammonia nitrogen in aquaculture wastewater to produce magnesium ammonium phosphate, which could then be used as fertilizer for resource recovery.

References

[1] Zhang, X., Fan, Y., Hao, T., Chen, R., Zhang, T., Hu, Y., Li, D., Pan, Y., Li, Y.Y., Kong, Z. Insights into current bio-processes and future perspectives of carbon-neutral treatment of industrial organic wastewater: a critical review. Environmental Research. 2024; 241: 117630.

[2] Chen, Y., Cheng, J.J., Creamer, K.S. Inhibition of anaerobic digestion process: a review. Bioresource Technology. 2008; 99(10): 4044-4064.

[3] Kong, Z., Li, L., Xue, Y., Yang, M., Li, Y.Y. Challenges and prospects for the anaerobic treatment of chemical-industrial organic wastewater: a review. Journal of Cleaner Production. 2019; 231: 913-927.

[4] Li, L.X., Yang, X.M., Li, A., Zhang, T., Liu, Y. Research progress of photosynthetic bacteria in wastewater treatment. Applied Mechanics and Materials. 2011; 71-78: 2831-2835.

[5] Luo, W., Deng, X., Zeng, W., Zheng, D. Treatment of wastewater from shrimp farms using a combination of fish, photosynthetic bacteria, and vegetation. Desalination and Water Treatment. 2012; 47(1-3): 221-227.

[6] Wang, H., Zhang, G., Peng, M., Zhou, Q., Li, J., Xu, H., Meng, F. Synthetic white spirit wastewater treatment and biomass recovery by photosynthetic bacteria: feasibility and process influence factors. International Biodeterioration & Biodegradation. 2016; 113: 134-138.

[7] Zhou, Q., Zhang, P., Zhang, G. Biomass and pigments production in photosynthetic bacteria wastewater treatment: effects of light sources. Bioresource Technology. 2015; 179: 505-509.

[8] Hülsen, T., Barry, E.M., Lu, Y., Puyol, D., Keller, J., Batstone, D.J. Domestic wastewater treatment with purple phototrophic bacteria using a novel continuous photo anaerobic membrane bioreactor. Water Research. 2016; 100: 486-495.

[9] Ponsano, E.H., Paulino, C.Z., Pinto, M.F. Phototrophic growth of *Rubrivivax gelatinosus* in poultry slaughterhouse wastewater. Bioresource Technology. 2008; 99(9): 3836-3842.

[10] Saejung, C., Thammaratana, T. Biomass recovery during municipal wastewater treatment using photosynthetic bacteria and prospect of production of single cell protein for feedstuff. Environmental Technology. 2016; 37(23): 3055-3061.

[11] Yang, A., Zhang, G., Yang, G., Wang, H., Meng, F., Wang, H., Peng, M. Denitrification of aging biogas slurry from livestock farm by photosynthetic bacteria. Bioresource Technology. 2017; 232: 408-411.

[12] Wang, Z., Torres, M., Paudel, P., Hu, L., Yang, G., Chu, X. Assessing the karst groundwater quality and hydrogeochemical characteristics of a prominent dolomite aquifer in Guizhou, China. Water. 2020; 12(9): 2584.

[13] Li, J., Zou, S.Z., Zhao, Y., Zhao, R.K., Zhou, C.S. Major ionic characteristics and factors of karst groundwater at Huixian Karst Wetland, China. Environmental Science. 2021; 42(4): 1750-1760.

[14] Li, B., Li, X.H., Peng, Q.X., Zhang, Q.M., Tang, S., Zhu, D.L., Plenković-Moraj, A., Sun, G. Characteristics of water color and its influencing factors in karst lakes of Huanglong Nature Reserve. Chinese Journal of Applied and Environmental Biology. 2022; 28(5): 1215-1224.

[15] Zhao, W., Zhang, G. Optimization of photosynthetic bacteria wastewater treatment and study of microbial species diversity. Desalination and Water Treatment. 2013; 52(28-30): 5357-5365.

[16] Yang, G., Lin, J., Zeng, E.Y., Zhuang, L. Extraction and characterization of stratified extracellular polymeric substances in *Geobacter* biofilms. Bioresource Technology. 2019; 276: 119-126.

[17] Bainor, A., Chang, L., McQuade, T.J., Webb, B., Gestwicki, J.E. Bicinchoninic acid (BCA) assay in low volume. Analytical Biochemistry. 2011; 410(2): 310-312.

[18] Smith, P.E., Krohn, R.I., Hermanson, G., Mallia, A., Gartner, F., Provenzano, M., Fujimoto, E., Goeke, N., Olson, B., Klenk, D. Measurement of protein using bicinchoninic acid. Analytical Biochemistry. 1985; 150(1): 76-85.

[19] Wang, Z., Wu, Z., Tang, S. Characterization of dissolved organic matter in a submerged membrane bioreactor by using three-dimensional excitation and emission matrix fluorescence spectroscopy. Water Research. 2009; 43(6): 1533-1540.

[20] Chen, W., Westerhoff, P., Leenheer, J.A., Booksh, K. Fluorescence excitation-emission matrix

regional integration to quantify spectra for dissolved organic matter. Environmental Science & Technology. 2003; 37(24): 5701-5710.

[21] Wang, K., Li, W., Gong, X., Li, Y., Wu, C., Ren, N. Spectral study of dissolved organic matter in biosolid during the composting process using inorganic bulking agent: UV–vis, GPC, FTIR and EEM. International Biodeterioration & Biodegradation. 2013; 85: 617-623.

[22] Guo, L., Lu, M., Li, Q., Zhang, J., Zong, Y., She, Z. Three-dimensional fluorescence excitation-emission matrix (EEM) spectroscopy with regional integration analysis for assessing waste sludge hydrolysis treated with multi-enzyme and thermophilic bacteria. Bioresource Technology. 2014; 171: 22-28.

[23] Sun, J., Guo, L., Li, Q., Zhao, Y., Gao, M., She, Z., Jin, C. Three-dimensional fluorescence excitation-emission matrix (EEM) spectroscopy with regional integration analysis for assessing waste sludge hydrolysis at different pretreated temperatures. Environmental Science and Pollution Research. 2016; 23(23): 24061-24067.

[24] Sheng, G.P., Yu, H.Q., Li, X.Y. Extracellular polymeric substances (EPS) of microbial aggregates in biological wastewater treatment systems: a review. Biotechnology Advances. 2010; 28(6): 882-894.

[25] Li, X.Y., Yang, S.F. Influence of loosely bound extracellular polymeric substances (EPS) on the flocculation, sedimentation and dewaterability of activated sludge. Water Research. 2007; 41(5): 1022-1030.

[26] Liao, B.Q., Allen, D.G., Droppo, I.G., Leppard, G.G., Liss, S.N. Surface properties of sludge and their role in bioflocculation and settleability. Water Research. 2001; 35(2): 339-350.

[27] Chai, L., Yan, X., Li, Q., Yang, B., Wang, X., Wang, Q. Enhancement of ZnO particles aggregation and sedimentation using polysaccharide and amino acid: importance in abiological granular sludge (ABGS) formation. Separation and Purification Technology. 2015; 151: 66-73.

[28] Mayer, C., Moritz, R., Kirschner, C., Borchard, W., Maibaum, R., Wingender, J., Flemming, H.C. The role of intermolecular interactions: studies on model systems for bacterial biofilms. International Journal of Biological Macromolecules. 1999; 26(1): 3-16.

[29] Higgins, M.J., Novak, J.T. Characterization of exocellular protein and its role in bioflocculation. Journal of Environmental Engineering. 1997; 123(5): 479-485.

[30] Liu, X.M., Sheng, G.P., Yu, H.Q. DLVO approach to the flocculability of a photosynthetic H_2-producing bacterium, *Rhodopseudomonas acidophila*. Environmental Science & Technology. 2007; 41: 4620-4625.

[31] Takahashi, M.M., Ichimura, S.E. Photosynthetic properties and growth of photosynthetic sulfur bacteria in lakes. Limnology and Oceanography. 1970; 15: 929-944.

[32] Mook, W.T., Chakrabarti, M.H., Aroua, M.K., Khan, G.M.A., Ali, B.S., Islam, M.S., Abu Hassan, M.A. Removal of total ammonia nitrogen (TAN), nitrate and total organic carbon (TOC) from aquaculture wastewater using electrochemical technology: a review. Desalination. 2012; 285: 1-13.